Universal cover-time distribution of heterogeneous random walks

Jia-Qi Dong [1,2] Wen-Hui Han [1] Yisen Wang [1] Xiao-Song Chen [3] and Liang Huang [1,*]
[1] *Lanzhou Center for Theoretical Physics and Key Laboratory of Theoretical Physics of Gansu Province, Lanzhou University, Lanzhou, Gansu 730000, China*
[2] *CAS Key Laboratory of Theoretical Physics, Institute of Theoretical Physics, CAS, Beijing 100190, China*
[3] *School of Systems Science, Beijing Normal University, Beijing 100875, China*

(Received 17 December 2021; accepted 24 January 2023; published 17 February 2023)

The cover-time problem, i.e., the time to visit every site in a system, is one of the key issues of random walks with wide applications in natural, social, and engineered systems. Addressing the full distribution of cover times for random walk on complex structures has been a long-standing challenge and has attracted persistent efforts. Usually it is assumed that the random walk is noncompact, to facilitate theoretical treatments by neglecting the correlations between visits. The known results are essentially limited to noncompact and *homogeneous* systems, where different sites are on an equal footing and have identical or close mean first-passage times, such as random walks on a torus. In contrast, realistic random walks are prevailingly *heterogeneous* with diversified mean first-passage times. Does a universal distribution still exist? Here, by considering the most general situations of noncompact random walks, we uncover a generalized rescaling relation for the cover time, exploiting the diversified mean first-passage times that have not been accounted for before. This allows us to concretely establish a universal distribution of the rescaled cover times for heterogeneous noncompact random walks, which turns out to be the Gumbel universality class that is ubiquitous for a large family of extreme value statistics. Our analysis is based on the transfer matrix framework, which is generic in that, besides heterogeneity, it is also robust against biased protocols, directed links, and self-connecting loops. The finding is corroborated with extensive numerical simulations of diverse heterogeneous noncompact random walks on both model and realistic topological structures. Our technical ingredient may be exploited for other extreme value or ergodicity problems with nonidentical distributions.

DOI: 10.1103/PhysRevE.107.024128

I. INTRODUCTION

Random walk [1–6] has been one of the pillars of the probability theory since the 17th century from the analysis of games of chance [7], and lays the foundation of the modern theory of stochastic processes and Brownian motions [8–10]. Cover time, the time for a random walker to visit all the sites, is a key quantity that characterizes the efficiency of exhaustive search [11–15]. The cover-time problem, also known as the traverse process [11,12], has widespread natural [16–19], social [14,15,20,21], and engineering [22–24] applications. Examples include rodent animals searching and storing as much food as possible in their confined habitats [16–18], the dendritic cells chasing all danger-associated antigens in a constantly changing tissue environment [19], collecting all the items in the classic coupon collector problem [14,15,20,21], the Wang-Landau Monte Carlo algorithm sampling every energy state in calculating the density of states in a rough energy landscape [22,23,25], robotic exploration of a complex domain for cleaning or demining and corresponding algorithm design [24], and information spreading or collecting on large scale Internet, mobile *ad hoc* network, peer-to-peer network, and other distributed systems where random walks are more feasible versus topology-driven algorithms due to the dynamical evolution, unknown global structure, limited memory, or otherwise broadcast storm issues [26–30].

Since the proposal of the cover-time problem [11–15], a series of theoretical progresses has been made for standard random walks, where the walker moves to the neighboring sites with equal probabilities. By bridging the cover time with the longest first-passage time (FPT, the time required to reach a particular site), the cover time can be estimated via the tail of the FPT distribution [14]. The average cover time scales distinctively in different dimensions, i.e., N^2 for one-dimensional lattices [13,15,31], $N(\ln N)^2$ for two-dimensional (2D) lattices with periodic boundary conditions or 2-torus [18,32], and $N \ln N$ for 3- or 4-torus [13].

Despite these theoretical progresses, the full distribution of the cover time for complex topologies has been a long-standing challenge and has attracted persistent efforts due to its ultimate importance in characterizing all types of statistics including extreme events [33–38]. Erdős and Rényi found in 1961 that the cover time for fully connected graphs with self-connecting loops (the coupon collection time) follows the Gumbel distribution [33], one of the well-known extreme value distributions [39]. Later in 1989 Aldous conjectured that for random walks on the $d \geqslant 3$ torus the distribution is also Gumbel [34], which has been proved by Belius in 2013 [35]. Recently, a substantial progress has been achieved for

*huangl@lzu.edu.cn

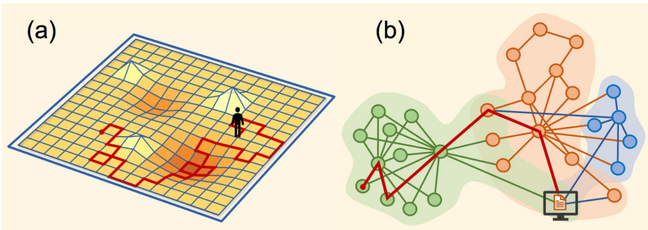

FIG. 1. Schematics of heterogeneous random walks. (a) Heterogeneity due to the confinement boundary and nonuniform landscapes, which result in diversified location-dependent occupation ratios and mean first-passage times. (b) Heterogeneity due to inherent heterogeneous connection structures, e.g., a small subset pruned from Wikipedia where nodes are pages and edges are hyperlinks.

noncompact *homogeneous* random walks, where the mean first-passage times (MFPTs) $\langle T_k\rangle \equiv \langle T_{k\leftarrow s}\rangle_s$ averaging over the starting sites are narrowly distributed and can be approximated by a single value $\langle T\rangle \equiv \langle T_k\rangle_k$, i.e., the global mean first-passage time (GMFPT). In particular, by rescaling the cover time τ as $\tilde{\chi} = \tau/\langle T\rangle - \ln N$ and employing the Laplace transform, the full distribution for $\tilde{\chi}$ was shown to follow the Gumbel universality class [36].

It should be noted that the theory in Ref. [36] only depends on a single value, i.e., the GMFPT $\langle T\rangle$, of different random walk models. This will be sufficient for *homogeneous* systems. For example, for random walks on a torus, $\langle T_k\rangle$ for different sites will be exactly the same due to the translational symmetry. However, for confined or disordered systems, or those with complex topological structures, as illustrated in Fig. 1, sites at different locations are obviously inequivalent [5,40–47], even in the thermodynamic limit. This invalidates the basis of the rescaling process and leads to an immediate question of whether there still exists a universal cover-time distribution for such systems, and more commonly, in general *heterogeneous* systems where $\langle T_k\rangle$ can be diverse [48]. This is of particular importance as most realistic systems are in fact heterogeneous.

In this paper, based on the transfer matrix framework and employing the longest FPT for the cover time, we derive the Gumbel universality class for rescaled cover-time distributions explicitly in heterogeneous systems under reasonable approximations. The key is the generalized rescaling relation exploiting the complete set of MFPTs $\{\langle T_k\rangle\}$, which can degenerate to Ref. [36] for homogeneous cases. Thus our results extend the universality of the Gumbel class to realistic, heterogeneous noncompact random walks. The finding is corroborated by extensive numerical simulations of 12 diverse random walk models with ideal or realistic heterogeneous structures, standard or biased random walk protocols, and undirected or directed connections.

The rest of the paper is organized as follows. In Sec. II, the distribution function of the rescaled cover times in heterogeneous systems is derived. Section III provides evidence of the universal distribution with extensive simulations. Conclusion and discussions are provided in Sec. IV. Detailed derivations are provided in the Appendixes.

II. THEORY OF UNIVERSAL COVER-TIME DISTRIBUTIONS FOR HETEROGENEOUS RANDOM WALKS

For random walks in homogeneous systems, different sites are on an equal footing where the MFPTs to all the sites are close to each other and can be approximated by their mean value, i.e., the GMFPT $\langle T\rangle$. In contrast, for random walks in a confined region, the existence of the boundary breaks the symmetry of the sites. For example, the boundary itself may have attracting effects that the walker crawls along the boundary and reaches sites closer to the boundary with a higher probability. Therefore, the FPT between a given pair of sites depends not only on their distance, but also on their specific locations. This is even critical for random walks on complex structures such as heterogeneous graphs, where sites with more edges are easier to be reached. As a natural consequence, the time for the walker to visit all the sites, i.e., the cover time, will need to consider the diversity of those FPTs, especially the long FPTs.

Therefore, in the following we shall first present the FPT distribution function based on the transfer matrix framework of Markovian process, which can take the heterogeneity into account through inhomogeneous transition probabilities. Then by counting the longest FPTs, the distributions of the cover times are derived.

A. First-passage time

The transfer probability that a random walker moves from site j to site i at the next time step given that in the current time step it is at site j is denoted as $\Omega_{i\leftarrow j}$. The case $i = j$ is included to account for the case when the walker has a nonzero probability to stay on the same site at the next time step, which effectively describes the effect of self-connecting loops. Collecting all the elements $\Omega_{ij} = \Omega_{i\leftarrow j}$ forms the transfer matrix $\mathbf{\Omega}$. The occupation probability $g_i(t)$ that a walker appears on site i at time t can be obtained recursively by

$$g_i(t) = \sum_j \Omega_{i\leftarrow j} g_j(t-1). \tag{1}$$

To obtain the FPT from starting site s to site k, a matrix $\mathbf{D}(k)$ is constructed based on Eq. (1). The element $D_{ij}(k)$ equals $\Omega_{i\leftarrow j}$ except the kth column $D_{ik}(k)$, which equals zero. When $\Omega_{i\leftarrow j}$ in Eq. (1) is replaced by $D_{ij}(k)$, if the random walker arrives at site k, it will be removed from the system in the next time step. Then, the FPT probability $F_{k\leftarrow s}(t)$ from site s to site k at time t is equal to the difference of the probability that the walker is still in the system at time t and that at $t+1$, given that the walker starts from site s in the beginning:

$$F_{k\leftarrow s}(t) = \|\mathbf{D}(k)^t \mathbf{G}(s)\|_1 - \|\mathbf{D}(k)^{t+1} \mathbf{G}(s)\|_1, \tag{2}$$

where $\mathbf{G}(s)$ is the initial spatial distribution at $t = 0$, $G_i(s) = 1$ if $i = s$ and zero otherwise, and $\|\mathbf{v}\|_1 = \sum_i v_i$ is the L1 norm of vector $\mathbf{v}$.

In very short time scales, $F_{k\leftarrow s}(t)$ is caused by the direct diffusion process according to the transfer matrix, thus it depends on the specific starting site s and could decrease rapidly versus time if s and k are not far from each other.

For large t, the asymptotic behavior of $F_{k\leftarrow s}(t)$ in Eq. (2) is determined by the largest eigenvalue λ_k $(0 < \lambda_k < 1)$ of the matrix $\mathbf{D}(k)$, i.e., $F_{k\leftarrow s}(t) \sim \lambda_k^t \sim e^{-t/T_k}$, where $T_k = -1/\ln(\lambda_k)$ is the characteristic FPT to site k in the long time limit. Therefore, the asymptotic behavior of Eq. (2) can be written as

$$F_k(t) \simeq \frac{1}{T_k} \exp\left(-\frac{t}{T_k}\right). \tag{3}$$

The FPT distribution $F_{k\leftarrow s}(t)$ in the long time limit only depends on T_k, but is independent of the starting site s. This is kind of surprising given here the context of heterogeneous random walks, which can be understood from the physical picture provided by Eq. (2). For a given target site k and a starting site s, there is a critical time scale, when the time is smaller than this critical time, it is mainly a diffusion process from the starting site to the other sites. The relative occupation probabilities on different sites will evolve into a steady state where they are proportional to the components of the eigenvector corresponding to the largest eigenvalue λ_k. This process depends on the starting site. Beyond that critical time scale, $F_{k\leftarrow s}(t)$ shrinks in time in the form of λ_k^t, where the relative occupation probabilities for different sites are fixed to be proportional to the components of the eigenvector of λ_k. That critical time scale can be very short compared to the FPTs. For example, assuming the second largest eigenvalue of $\mathbf{D}(k)$ is λ_k', then the weight of the second largest eigenvector over the largest one decays in time as $(\lambda_k'/\lambda_k)^t$, thus this critical time can be in the order of tens or hundreds compared with tens of thousands or hundreds of thousands for typical FPTs. See Appendix A for a detailed numerical example for Eq. (3). For random walk on homogeneous systems such as lattices with periodic boundary conditions, all target sites are identical and share the same characteristic FPT. However, for heterogeneous systems such as confined regions with nontrivial boundary conditions or other complex structures, the characteristic FPT T_k can be scattered in a broad span, thus the distribution function $F_k(t)$ will be nonidentical and site dependent. Therefore, the complete set of the diverse characteristic FPTs will be needed to determine the cover-time distribution in heterogeneous system.

In many cases it is impractical to calculate the characteristic FPT T_k based on matrix $\mathbf{D}(k)$, since the transfer probability $\Omega_{i\leftarrow j}$ cannot be completely obtained in general. Alternatively, since $T_k = \int tF_k(t)dt$ is also the mean FPT to site k, T_k can be approximated by the average of the FPT $T_{k\leftarrow s}$ from all possible starting sites s to site k, i.e., $T_k \approx \langle T_k\rangle \equiv \langle T_{k\leftarrow s}\rangle_s$ (see Appendix A for an exemplary numerical verification), which can be calculated more efficiently.

B. Full cover time

For a trajectory which fully covers the system, the random walker will first successively pass $N-1$ sites in a specific order. Then the time arriving at the last unvisited site is the full cover time. Meanwhile, this time is also the FPT to this ending site. Therefore, the cover time can be regarded as the longest FPT in a single cover process [14]. As a result, ignoring the correlations between the visits, the probability that the cover time equals τ can be estimated as

$$P(\tau) = \frac{1}{N}\sum_{k,s,\ k\neq s} F_k(\tau)\left[\prod_{i\notin\{k,s\}}\sum_{t=1}^{\tau-1} F_i(t)\right], \tag{4}$$

where $\sum_{t=1}^{\tau-1} F_i(t)$ is the probability of the first arrival onto the site i up to time $\tau-1$, which is exactly the probability that this site i will be visited during the first $\tau-1$ steps. The product over i in the square brackets is thus the probability that all sites, except s and k, are visited up to $\tau-1$, as if they were realized by independent walkers. $F_k(\tau)$ is the probability that the last unvisited site k is first visited at τ, which completes the covering process. The factor $1/N$ is for the average over all the starting sites. Equation (4) neglects any structural correlation of the background system, which should be (at least weakly) satisfied for noncompact random walks [49], i.e., the diffusion dimension d_w of the random walk (defined by $\langle|\mathbf{r}|^2\rangle \sim t^{2/d_w}$) is smaller than the dimension of the background space d. In this case, the number of sites visited by the walker $|\mathbf{r}|^{d_w}$ will be negligible compared to all the sites within $|\mathbf{r}|$, which is $|\mathbf{r}|^d$. Thus the walker needs to traverse the region many times in order to cover all the sites. This means that the effective structural correlation will be significantly reduced as the information of the initial position is completely lost when the walker comes back again.

Replacing T_k by $\langle T_k\rangle$, and considering $\tau - 1 \cong \tau$ for $\tau \gg 1$, the summation in the square bracket yields

$$\sum_{t=1}^{\tau} F_k(t) \cong 1 - \exp\left(-\frac{\tau}{\langle T_k\rangle}\right). \tag{5}$$

For τ being large, higher order terms in the product in the square bracket can be neglected, leading to

$$\prod_{i=1}^{N}\sum_{t=1}^{\tau} F_i(t) \cong \exp\left[-\sum_{i=1}^{N}\exp\left(-\frac{\tau}{\langle T_i\rangle}\right)\right], \tag{6}$$

where the condition $i \notin \{k, s\}$ has also been relaxed. Define a rescaled cover time χ from the original cover time τ by

$$\chi = -\ln\sum_{i=1}^{N} e^{-\frac{\tau}{\langle T_i\rangle}}, \tag{7}$$

where the summation can be replaced by the integration if the distribution of $\langle T_i\rangle$ is known, i.e., $\sum_i e^{-\frac{\tau}{\langle T_i\rangle}} = N\int e^{-\frac{\tau}{\langle T_i\rangle}} P(\langle T_i\rangle)d\langle T_i\rangle$. Practically, when the topological structure and the type of random walks are known, the distribution $P(\langle T_i\rangle)$ can be obtained via Monte Carlo simulation. Together with Eq. (3), it is straightforward to show that $\sum_k F_k(\tau) = \exp(-\chi)d\chi/d\tau$. Thus one has

$$P(\tau)d\tau \cong \exp[-\exp(-\chi)]\exp(-\chi)d\chi, \tag{8}$$

yielding a universal distribution function for the rescaled cover time χ that is independent of any of the system details:

$$P(\chi) = \exp[-\chi - \exp(-\chi)]. \tag{9}$$

The detailed derivations are shown in Appendix B.

Equation (9) is the Gumbel distribution which is one of the three well-known extreme value distributions [50], and shares the same form as in the theory for homogeneous cases

[36]. The main difference is the rescaling functional relation between χ and τ, e.g., $\tilde{\chi} = \tau/\langle T \rangle - \ln N$ for homogeneous cases, and Eq. (7) for the heterogeneous cases, which now requires the complete set of MFPTs $\{\langle T_k \rangle\}$ or their distribution function. Equation (7) ensures a monotonous relation between χ and τ. For homogeneous cases, all sites share a single identical characteristic MFPT, which is then the GMFPT $\langle T \rangle$, and Eq. (7) degenerates to $\tilde{\chi} = \tau/\langle T \rangle - \ln N$.

Note that in the derivation of Eq. (9), it is assumed that the cover time is large compared to the MFPT $\langle T_k \rangle$. This condition is typically satisfied automatically, as the cover time τ ending at site k is approximately the longest FPT to k. Therefore, the large FPT dominates in the covering process, justifying the use of Eq. (3). Even for short τ, e.g., negative χ, it is usually still larger than $\langle T_k \rangle$, thus Eq. (9) works well.

C. Partial cover time

For a random walk in which the walker only needs to visit a fraction of the system, it is obvious that the time cost depends on how to choose the unvisited sites. There are two related processes: one is random cover, and the other is partial cover. In the random cover problem, the m sites that are not counted (but can be visited) are chosen randomly from the total N sites in the system before the cover process. For $m \ll N$, due to the noncompact nature of the random walk, the walker needs to traverse the system many times in order to visit all the sites, thus any site in the system will be visited many times on average. For example, for homogeneous random walk, the most probable rescaled cover time is $\tilde{\chi} = 0$, yielding $\tau = \langle T \rangle \ln N$, where $\langle T \rangle$ is typically in the order of N or even larger. For a system with $N = 1000$ sites, each site will be visited $\ln N \approx 7$ times for typical covering processes, including those uncounted sites. Therefore, if m is small, the uncounted sites are most likely to be already visited during the random cover process when the rest of the system is covered. Therefore the random cover will have almost the same cover-time distribution with the full cover process. In the partial cover process, it stops when there are m sites left. If the m sites are distributed randomly in the system, for the full cover process the walker needs to wander over the system again and again until it finds all of them, which will in general take a much longer time, at least in the order of their respective MFPTs. Therefore, the partial cover times will have a nontrivial distinctive distribution other than that for random or full cover processes.

Although significantly different from the full cover process, for partial cover there still exists a universal distribution for noncompact random walks in heterogeneous systems. In particular, the partial cover-time distribution can be expressed as

$$P_m(\tau) = \sum_{\{I_m\}} P(\tau | \notin \{I_m\})\, Q(\tau, \{I_m\}), \tag{10}$$

where $\{I_m\}$ is a specific set of m sites, and we assume $m \ll N$. The first term $P(\tau | \notin \{I_m\})$ denotes the probability that the walker visits the $N - m$ other sites during time τ regardless of the sites in the set $\{I_m\}$ being visited or not. This follows the random cover-time distribution, which can be approximated by the full cover-time distribution.

The second term $Q(\tau, \{I_m\})$ is the probability that the sites in set $\{I_m\}$ are not visited yet at time τ. If the unvisited sites $\{I_m\}$ are independent, i.e., the information of the sites that are already visited in $\{I_m\}$ does not change the probability that any of the rest of the sites in $\{I_m\}$ will be visited, the second term Q can be simplified as

$$Q(\tau, \{I_m\}) = \prod_{i\in\{I_m\}} \left(1 - \sum_{t=1}^{\tau} F_i(t)\right) = \prod_{i\in\{I_m\}} \exp\left(-\frac{\tau}{\langle T_i \rangle}\right),$$

where the second equality makes use of Eq. (5).

After enumerating all possible configurations of $\{I_m\}$ by the summation $\sum_{\{I_m\}}$, the partial cover-time distribution $P_m(\tau)$ can then be obtained in the form of Gumbel class (Appendix C)

$$P_m(\chi) = \frac{1}{m!} \exp[-(m+1)\chi - e^{-\chi}], \tag{11}$$

where χ is the rescaled cover time and is defined by Eq. (7). Equation (11) has the same form as that given in Ref. [36] for homogeneous cases. According to Eq. (11), the most probable rescaled partial cover time χ^* satisfies $\exp(-\chi^*) = 1 + m$, or $\chi^* = -\ln(1 + m)$. Thus χ^* is characteristically distinct for different m. Due to the monotonous relation between χ and τ, this indicates that the corresponding characteristic times τ^* to visit N ($m = 0$) and $N - 1$ ($m = 1$) sites are discontinuous, which is consistent with the results in Ref. [51] for full cover and partial cover with $m = 1$ in 2D lattices.

For correlated unvisited sites, since $P(\tau | \notin \{I_m\})$ is approximately the random (or full) cover-time distribution, the main issue caused by the correlation is the simplification of the Q term. When $N \gg m$, the correlation of the unvisited sites can be weak, and it will lead to only a small correction. As a consequence, m will need to be replaced with an effective, typically smaller, m^*, and the rescaled partial cover-time distribution has the same form as Eq. (11). Indeed, it has been found that for various heterogeneous random walk models, the rescaled partial cover-time distributions of different systems can collapse to an identical distribution function that agrees perfectly with Eq. (11). However, there are also cases that correlation of unvisited sites could be so strong that it cannot be ignored even in the large N limit, especially for low dimensional random walks, such as 2D persistent random walks and random walk on three-dimensional (3D) lattices with reflective boundaries.

D. Parallel search

Parallel search is an important practical issue when there are n ($\ll N$) independent walkers. The system is covered when each site is visited at least by one of the walkers. We have examined the MFPT and the rescaled cover-time distribution in heterogeneous systems. In particular, in the long time limit, the MFPT to site k follows n independent and identical distributions of Eq. (3), which is then $F_k^{(n)}(t) \simeq \frac{n}{T_k} e^{-\frac{nt}{T_k}}$. Thus the new characteristic FPT T_k' (also the MFPT $\langle T_k' \rangle$) becomes $1/n$ of that for one walker. With the new set of $\{\langle T_k' \rangle\}$, the rescaled cover time can be obtained from Eq. (7) to yield the universal distributions Eqs. (9) and (11). Thus when there are n independent parallel walkers in a heterogeneous system, the cover time will be $1/n$ as that for one walker. This result has been found in Ref. [36] for homogeneous cases, it is kind of surprising that it is also the case for heterogeneous random walks. This is because the distribution of the MFPTs to a particular site k in the circumstance of n independent walkers has the same form with only the characteristic time divided by n.

III. NUMERICAL VERIFICATION

A. Generality and the random walk models

It should be noted that our approach to derive the full and partial cover-time distribution is based on the general framework of transfer matrix, whose elements can be assigned arbitrarily given the normalization condition that the summation of the elements for each column is 1. It is not necessary that the walker moves to the neighbors with equal probability as in the standard random walk models. Indeed, the results are also valid for biased walking protocols or directed connections, as will be demonstrated in the simulation part. In addition, the walker may have a nonzero probability to stay on the same site for the next step, accounting for the self-connecting loop effects. These considerations enable our theory to be applicable in broad realistic circumstances.

In this section, the universality of the rescaled cover-time distribution will be corroborated with different types of random walks on various heterogeneous systems, for both full cover [Eqs. (9) and (7)] and partial cover [Eqs. (11) and (7)] processes. Here we provide extensive numerical simulation results for 12 cases with different random walk models and topological structures, including three realistic networks, which agree with the full cover theory well. For partial cover, most of the simulation cases (10) agree, but deviation occurs for low dimensional cases where the correlation of the unvisited sites is not negligible.

The 12 random walk cases are (1) standard random walk on a 3D lattice with reflective boundaries (SRW 3D); (2) standard random walk on a four-dimensional (4D) lattice with reflective boundaries (SRW 4D); (3) standard random walk on an Erdős-Rényi (ER) graph (SRW ER); (4) standard random walk on scale-free graphs (SRW SF); (5) biased random walk on an Erdős-Rényi graph (BRW ER); (6) biased random walk on scale-free graphs (BRW SF); (7) persistent random walk on a 2D lattice with reflective boundaries (PRW 2D); (8) the Lévy flight on a 2D lattice with sticking boundaries (LF 2D); (9) chaotic motion as random walks (Logistic); (10) standard random walk on the Internet at the autonomous system level (Internet); (11) standard random walk on the Twitch social network (Twitch); and (12) standard random walk on the directed subgraph containing the page "Random walk" of Wikipedia (Wiki). The topological structures of the last three cases come from the real-world complex systems. These models are chosen due to their simplicity, representativeness, and significance in realistic applications.

In our simulation, a site s is chosen randomly from a total of N sites with probability $1/N$ as the starting site, then the random walk begins, until it covers the whole system, yielding the cover time τ. In the meantime, the partial cover time with arbitrary m and one ensemble of the FPT from the starting site s to all the other sites k, $T_{k\leftarrow s}$, are also obtained. For each

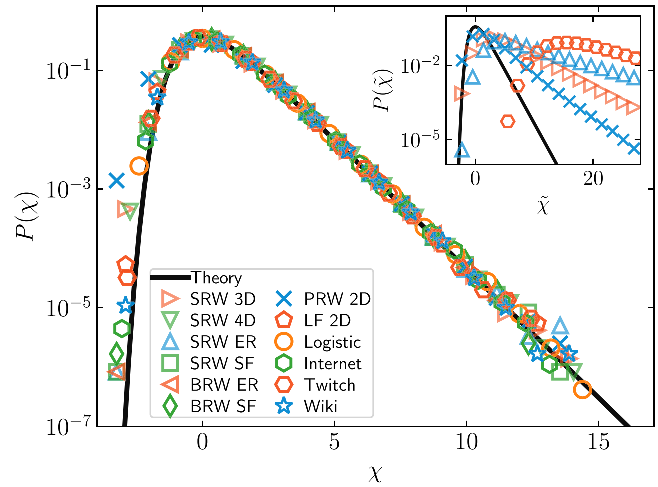

FIG. 2. Rescaled full cover-time distributions of the 12 random walk cases. The key parameters are as follows. SRW 3D, $N = 343$; SRW 4D, $N = 625$; SRW ER, $N = 1000$, $\langle K\rangle = 8$; SRW SF, $N = 2000$, $\langle K\rangle = 4$; BRW ER, $N = 1000$, $\langle K\rangle = 8$; BRW SF, $N = 2000$, $\langle K\rangle = 4$; PRW 2D, $N = 2304$, $l_c = 24$; LF 2D, $N = 1600$; Logistic, $N = 1000$; Internet, $N = 11\,174$; Twitch, $N = 7126$; Wiki, $N = 3623$. The cover-time distribution for each case is evaluated from sampling over 1×10^6 rounds. The symbols are the data rescaled with Eq. (7), and the thick black curve is Eq. (9). Inset: A few representative cases where the cover time is rescaled based only on the GMFPT as $\tilde{\chi} = \tau/\langle T\rangle - \ln N$. The thick black curve is the corresponding prediction.

case, 1×10^6 rounds by randomly choosing s are carried out to obtain reliable statistics. Then for each site k, averaging over the starting site s for the 1×10^6 rounds of $T_{k\leftarrow s}$ yields the MFPT $\langle T_k\rangle$, and thus the MFPT set $\{\langle T_k\rangle\}$ for all the sites. For each cover time τ, the corresponding χ is derived according to Eq. (7) based on the numerically obtained MFPT set $\{\langle T_k\rangle\}$. Then the distribution of the 1×10^6 χ values is obtained by direct counting, which is plotted in Fig. 2. The different symbols are for different cases. They are all in good agreement with the universal distribution Eq. (9) as plotted by the thick black curve.

All the above 12 cases are heterogeneous. Due to the diversified value of the MFPT $\langle T_k\rangle$, the GMFPT $\langle T\rangle$ is insufficient to rescale the cover time by $\tilde{\chi} = \tau/\langle T\rangle - \ln N$, which leads to substantial deviations, as shown in the inset of Fig. 2 for a few representative cases.

A brief description of the models is as follows. Detailed parameters may be listed in the caption of the corresponding figures.

(1) Standard random walk on a 3D lattice in a cubic domain with reflective boundary conditions (SRW 3D), i.e., if the walker moves outside the boundary, it will be reflected back to the cubic domain. As a result, the MFPT to the target site is location dependent and mainly depends on the distance to the boundary [41,47,52]. For a given finite domain, the transfer matrix $\mathbf{\Omega}$ can be written down explicitly [53].

(2) Standard random walk on a 4D lattice in a hypercubic domain with reflective boundary conditions (SRW 4D). The transfer matrix $\mathbf{\Omega}$ can be obtained similarly.

(3) Standard random walk on an Erdős-Rényi graph [54] (SRW ER). The ER graph with size N is generated by connecting each pair of nodes with probability p. A graph is connected if there is always a path passing through sites and edges to connect any given pair of sites. In our simulation, only the connected graphs are considered. The degree K of a site is the number of its edges. The degree distribution for the ER graph is Poissonian: $P(K) = \frac{\langle K\rangle^K}{K!}\exp(-\langle K\rangle)$, where $\langle K\rangle \approx Np$ for large N is the average degree, which is also the variance. Thus when $\langle K\rangle$ is large, the relative standard deviation with respect to the mean, i.e., $1/\sqrt{\langle K\rangle}$, is small, and the system is approximately homogeneous. However, when $\langle K\rangle$ is not so large, the degrees and consequently the MFPTs can be broadly distributed, breaking the homogeneous assumption. In this paper we choose $\langle K\rangle = 8$, where the heterogeneity is obvious, and consider those only connected graphs to carry out random walk simulations.

For standard random walk on a graph, starting from any site with degree K, the walker moves to any of its neighboring sites with equal probability $1/K$.

(4) Standard random walk on scale-free graphs (SRW SF) with power law degree distribution [55], i.e., $P(K) \sim K^{-\gamma}$ and $\gamma = 3$ in our simulation, where $\langle K\rangle = \int KP(K)dK = 4$ is the average degree. This system is inherently heterogeneous, even in the thermodynamic limit.

(5) Biased random walk on an Erdős-Rényi graph (BRW ER). Unlike the standard random walk in which the walker moves to one of its neighbors with equal probability, for a biased random walk, the walker at site s with K_s neighbors moves to a neighboring site i with the probability $K_i^{-\alpha}/\sum_{j=1}^{K_s} K_j^{-\alpha}$, where the summation is over the site i's neighbors. When $\alpha = 0$, it returns to the standard random walk. We take $\alpha = 1$ for this case. $\langle K\rangle = 8$.

(6) Biased random walk on scale-free graphs (BRW SF) with $\langle K\rangle = 4$, $\alpha = 0.18$.

(7) The persistent random walk [56,57] on 2D lattices in a square domain of side length L with reflective boundary conditions (PRW 2D). The walker keeps its previous moving direction with probability p_r, and moves to any of the other three directions with probability $(1 - p_r)/3$. The mean persistent length is given by $l_c = 1/(1 - p_r)$ [56]. When it is much larger than 1, the random walk is noncompact. However, when l_c is small, especially when $l_c \approx 1.3$, the persistent random walk degenerates to conventional random walk, which becomes compact. In addition, the persistent random walk is not Markovian, i.e., it not only depends on the current position, but also depends on its previous step, therefore the transfer matrix framework is valid only approximately, leading to deviations from the theory, especially for the short cover times (negative χ).

(8) The Lévy flight [17,58–61] on 2D lattices in a square domain of side length L with sticking boundaries (LF 2D). The walker flies in one of the four directions $(\pm x, \pm y)$ to a site of distance l with probability $P(l) = \frac{1}{\pi}\int_{-\infty}^{\infty}\exp(-l_0^a k^a)\exp(ikl)dk$ [36], where $l_0 = L/20$ and $a = 3/2$ are constants. If the walker flies out of the region at one time step, it will be stuck at the boundary along its flying route, and continues the flight at the next step.

(9) Chaotic trajectories as a biased and directed random walk (Logistic), which is biased and directed due to the dynamical structures. A feature for chaotic dynamical systems is that an initial perturbation $\delta(0)$ will be enlarged exponentially in time, i.e., $\delta(t) = \delta(0)\exp(h_1 t)$, where the largest Lyapunov exponent h_1 is positive, and $1/h_1$ is the Lyapunov time. The predictability of the chaotic trajectory will vanish after evolving a few Lyapunov times [62,63]. Therefore, in time scales that are much larger than the Lyapunov time, the chaotic trajectory can be regarded as a stochastic process. An interesting question is whether the time for the chaotic trajectory to cover the coarse-grained phase space (the coarse-grained ergodic time) also obeys the universal cover-time distribution. Here we take the fully chaotic logistic map as an example, which is $y_{n+1} = 4y_n(1 - y_n)$. The system is ergodic and the entire phase space can be filled if the evolution time is long enough. The region [0,1] of the map is divided into N mesh grids. Since the grids have a non-negligible finite size $1/N$, although the original dynamics is deterministic, due to the chaotic nature, the trajectory on the scale of the grids can be highly stochastic. The occupation ratio is proportional to the natural measure of the system and is highly nonuniform for the logistic map [64]. This suggests that the MFPT $\langle T_k\rangle$ should be also diverse and depends on the position of target grid k.

(10) Standard random walk on the Internet at the level of autonomous systems (Internet). This undirected connection structure is a snapshot in 2001 which contains 11 174 nodes and 23 409 edges [65].

(11) Standard random walk on a subset of the Twitch social network (Twitch). A node is a Twitch user who streams in English, and an edge between two users represents their mutual friendship. This social network contains 7126 users and 35 324 edges [66].

(12) Standard random walk on a directed subgraph of Wikipedia (Wiki). The subgraph is pruned from the hyperlink network of Wikipedia, where the original data set is provided in Refs. [67,68]. The node is the page in Wikipedia, and a directed edge represents a hyperlink from one page to another. The original data set has about 4×10^6 nodes and 100×10^6 links, which is far beyond our computation power. Therefore, we extract a smaller cluster in which any page can be reached by following at most two steps from the page "Random walk." This cluster is strongly connected, in that for each pair of nodes (i, j), there always exists a directed path in the cluster going from i to j. This subgraph contains 3623 nodes and 75 929 directed edges. The walker moves randomly along the directed edge, which simulates a wanderer exploring Wikipedia. The probability that the walker moves to a neighboring node (page) is $1/K_o$, where K_o is the out-degree of the current node.

B. Numerical verification for full, partial, and parallel cover processes

The rescaled cover-time distributions for all the 12 cases are plotted in Fig. 2. Despite the diversity of the random walk models, the background topology, the biased protocols, and the directed links, the simulation results all fall onto the theoretical curve well, especially for positive χ values. As a comparison, the distributions of the rescaled cover time based only on the GMFPT ($\tilde{\chi} = \tau/\langle T\rangle - \ln N$) for a few

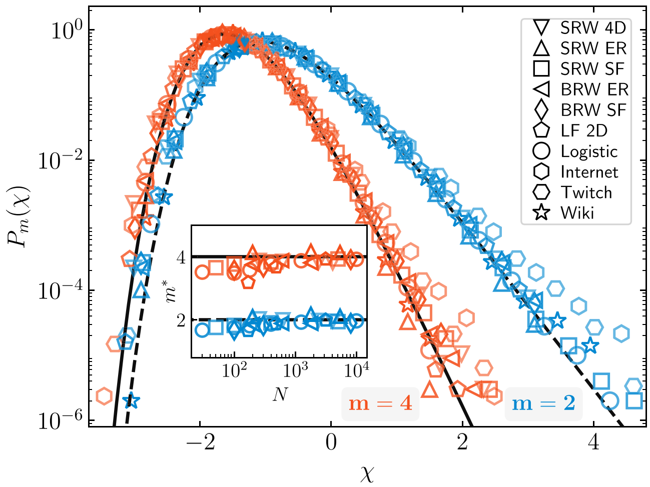

FIG. 3. Rescaled partial cover-time distributions of ten heterogeneous random walk models as labeled in the figure. SRW 4D, $N = 4096$; SRW ER, $N = 5400$; SRW SF, $N = 5000$; BRW ER, $N = 5400$; BRW SF, $N = 2000$; LF 2D, $N = 6400$; Logistic map, $N = 10\,000$; Internet, $N = 11\,174$; Twitch, $N = 7126$; and Wiki, $N = 3623$. Each distribution is obtained from 1×10^6 samples. The symbols are the data, and the curves are the theory Eq. (11) for $m = 2$ (dashed) and $m = 4$ (solid). The inset shows the effective m^* vs size N of the seven model systems where the size can be changed.

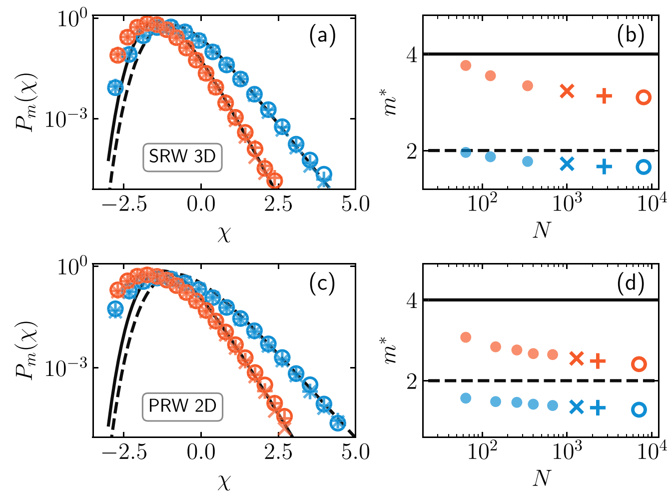

FIG. 4. (a) Rescaled partial cover-time distribution of SRW 3D. $N = 1000, 2744, 8000$ for crosses, pluses, and circles, i.e., the three data points with the largest size in (b). The dashed curve is Eq. (11) with $m^* = 1.7$ for $m = 2$, and the solid curve is $m^* = 3.1$ for $m = 4$. (b) The effective m^* vs size N for SRW 3D. (c) Rescaled partial cover-time distribution of PRW 2D. $N = 1296, 2304, 7056$ for crosses, pluses, and circles. The dashed curve is Eq. (11) with $m^* = 1.3$ for $m = 2$, and the solid curve is $m^* = 2.5$ for $m = 4$. (d) The effective m^* vs size N for PRW 2D. The characteristic persistent length is $l_c = L/2$.

representative cases, e.g., standard random walks in confined 3D lattices, the ER graph, Twitch, and persistent random walks on confined 2D lattices, are shown in the inset of Fig. 2. They deviate from the prediction significantly. This illustrates that for heterogeneous systems, rescaling of the cover time only using the GMFPT is insufficient, and the complete set of MFPTs is needed to properly rescale the cover time.

For partial cover time, the correlation effects are more significantly revealed, and the 12 heterogeneous random walk models can be classified into two groups. The second group consists of two cases: the standard random walk on 3D lattices and persistent random walk on 2D lattices with reflective boundaries. The remaining ten cases are the first group, where the correlation between the unvisited sites is small. The rescaled partial cover-time distributions of these ten systems are shown in Fig. 3, which agree well with the theoretical prediction Eq. (11). The correlation between unvisited sites can be treated by a modified value of m, i.e., m^*, in Eq. (11), which can be obtained by fitting the data to the curve Eq. (11). The difference between m^* and m then characterizes the extent of correlation. The inset of Fig. 3 shows the dependence of m^* on the system size. It can be seen that the overall values of m^* are close to m, and as the system size increases, m^* converges to m. This is consistent with the expectation that as the size of the system increases, the correlation between the unvisited sites decreases.

For the second group, they are both low dimensional cases, where correlation between unvisited sites could be non-negligible and leads to a larger difference between m^* and m. The rescaled cover time and the dependence of m^* versus system size for these two cases are shown in Fig. 4. With the effective m^*, the rescaled partial cover-time distribution again follows Eq. (11) reasonably well, especially in the large cover time limit [Figs. 4(a) and 4(c)]. However, in contrast to the first group, here m^* is close to m only for small system sizes. As the system size increases, the difference between m^* and m does not vanish; instead it becomes larger and m^* approaches to a constant but smaller value than m, as shown in Figs. 4(b) and 4(d). Given the behavior of the data, this effect is expected to persist even in the thermodynamic limit. Furthermore, as shown in Fig. 4(c), for each m, the cover time for systems with different size can still be rescaled to follow the same distribution, as the data points collapse on each other in almost all χ ranges, although the deviation from Eq. (11) at negative χ is apparent. This indicates that although the "real" rescaled distribution function for partial cover time might be different from the theoretical expectation, the scaling relation Eq. (7) still holds.

For parallel search, when there are n independent walkers, the new MFPT $\langle T_k' \rangle$ becomes $1/n$ of that for one walker. With the new set of $\{\langle T_k' \rangle\}$, the rescaled cover time can be obtained from Eq. (7) to yield the universal full and partial cover-time distributions Eqs. (9) and (11). Here we provide numerical evidence for the validity of the above reasoning. Figure 5 shows the results of both the full and the partial cover-time distributions when there are five independent walkers in the simulation systems. It is clear that the distributions from the simulation agree with the theoretical curves well.

IV. DISCUSSIONS AND CONCLUSION

The full distribution of cover time for random walks on complex topological structures has been a long-standing issue with broad potential applications. It has been found widely and robustly in various *homogeneous* noncompact random

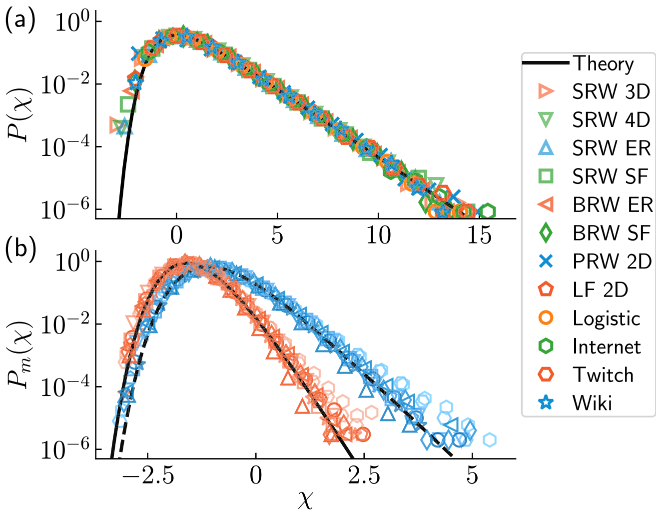

FIG. 5. The cover-time distribution when there are five independent walkers for the simulation models. (a) The full cover-time distribution of the 12 systems in Fig. 2. (b) The partial cover-time distribution of the ten systems in Fig. 3 with dashed and solid lines for $m = 2$ and 4, respectively.

walk models that the cover times can be rescaled to follow the Gumbel distribution [33–37]. These results assume that the MFPTs are identical or close to each other. However, in realistic systems such as confined domains or those with inhomogeneous components [5,40–47,69–73], heterogeneity is prevailing, leading to broad spans of the MFPT values [48,74].

In this paper, based on the transfer matrix framework, we have established the universal distribution in *heterogeneous* noncompact random walks for both full and partial cover processes. Our results show that the rescaled cover times fall again onto the Gumbel universality class. Thus we step forward and ground the Gumbel universality of the cover-time distribution on a much broader field of random walks that are prevalent in realistic circumstances. The key is the rescaling relation, Eq. (7), where the complete set of the MFPTs $\{\langle T_k\rangle\}$ or their distribution is needed to account for their diversified values. The results have been corroborated by extensive numerical simulations on 12 random walk models with various background topologies. Thus our approach is valid for generalized random walks that can be either standard or biased, undirected or directed, and can have self-connecting loops.

Note that the requirement of noncompactness is crucial to our results for both full and partial cover processes. Actually, it is the most common requirement to develop theories for cover-time distributions, as only for noncompact random walks the correlation can be ignored, and the probability approach can be tackled straightforwardly. For compact random walks, the correlation cannot be ignored, thus our approach becomes invalid. Nevertheless, as Figs. 4 and 8 show, when there is non-negligible correlation, the deviation from the theory is mostly in the small or negative χ range. This is comprehensible as only for small or negative χ where the cover time is short the correlation between subsequent visits is strong due to the spatial lattice structure that can be attributed to the low dimensionality, i.e., the walker has a much higher probability to visit its neighbors than distant sites. For large positive χ, long cover time indicates that the walker will traverse the lattice many times before a full cover is accomplished, which is analogous to noncompact walk, leading to good agreement with the Gumbel distribution.

Since heterogeneity is prevailing in realistic random walk situations, e.g., either due to the spatial confinement on the 2D terrestrial surface or in three dimensions by the cell membrane, building structure, etc., or due to the inherent heterogeneity in the social and engineered systems, our results are expected to have broad applications. For example, our results can be used as a guideline in the design of searching or demining algorithms of robots in complicated environments, or control of the exhaustive information collecting or broadcasting in heterogeneous cyberspace or constantly evolving distributed sensing and communicating systems.

As our theory solves the distribution function of the extreme value problems with nonidentical distributions, it may be exploited in investigating other extreme value problems such as extreme climate events, robustness of engineered systems, etc. [39,75–77], with heterogeneous characteristic spatial or time scales. In addition, the cover process of chaotic trajectories in discretized phase space is effectively the ergodicity issue. Thus our treatment can also be used to estimate the ergodic time of chaotic dynamical systems for a given discretization (or observation resolution) of the phase space with nonuniform natural measures.

ACKNOWLEDGMENTS

This work is supported by National Natural Science Foundation under Grants No. 12175090, No. 11775101, No. 11905087, No. 12135003, and No. 12047501, the 111 Project under Grant No. B20063, and by China Postdoctoral Science Foundation under Grant No. 2019M660810.

APPENDIX A: FPT DISTRIBUTION AND APPROXIMATION OF T_k BY $\langle T_k\rangle$

In general, the exponential form in Eq. (3) of the distribution of the FPTs to site k is valid only for large FPTs; therefore, it can be written more accurately as in the large FPT limit

$$F_k(t) \sim c_k \exp\left(-\frac{t}{T_k}\right), \tag{A1}$$

where c_k is a constant. Then the summation of Eq. (5) for $\tau \gg 1$ becomes

$$\sum_{t=1}^{\tau} F_k(t) \cong 1 - \int_{\tau}^{\infty} F_k(t)dt = 1 - c_k T_k \exp\left(-\frac{\tau}{T_k}\right). \tag{A2}$$

The coefficient $c_k T_k$ will enter into Eqs. (6) and (7) for the rescaling relation, i.e.,

$$\chi = -\ln \sum_{i=1}^{N} c_i \langle T_i\rangle e^{-\frac{\tau}{\langle T_i\rangle}}, \tag{A3}$$

where T_i has been replaced with $\langle T_i\rangle$ for convenience.

The coefficients $c_i\langle T_i\rangle$ will render the calculation much more difficult. Fortunately, as demonstrated in Fig. 6, $F_k(t)$

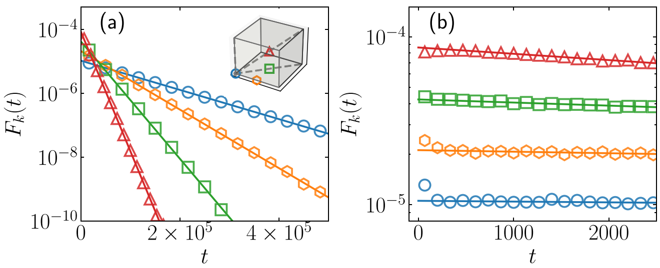

FIG. 6. For standard random walk on a cube of 3D lattice with $L = 21$ and reflective boundary conditions. (a) The distribution of FPTs to a few representative sites marked in the inset, i.e., corner, edge center, face center, and body center for circles, hexagons, squares, and triangles, respectively. (b) A zoom-in of (a) for $t < 3000$. The curves are Eq. (3) with $T_k = 94\,891.5, 47\,415.5, 23\,582.9$, and $11\,594.5$, respectively, as computed from $\mathbf{D}_k$.

starts to follow a perfect exponential distribution for $t \ll T_k$, around $0.01T_k$ or even $0.001T_k$. Therefore, $F_k(t)$ can be approximated by the exponential distribution well almost in the whole range, leading to $c_k = 1/T_k$ by the normalization condition. The coefficient $c_i\langle T_i\rangle = 1$, and Eq. (A3) reduces to Eq. (7).

Figure 7 compares the MFPT $\langle T_k\rangle$ and the characteristic FPT T_k of standard random walk for representative sites in a cube of a 3D lattice with reflective boundary conditions. Figure 7(a) shows that both $\langle T_k\rangle$ and T_k almost overlap. Figure 7(b) plots the relative difference, i.e., $|\langle T_k\rangle - T_k|/T_k$. It is clear that the relative difference is within 2%, indicating that the approximation of T_k by $\langle T_k\rangle$ is valid.

APPENDIX B: DERIVATION OF THE RESCALED FULL COVER-TIME DISTRIBUTION

For the noncompact random search process, the cover-time distribution can be estimated by Eq. (4), i.e.,

$$P(\tau) = \frac{1}{N}\sum_{k,s,\ k\neq s} F_k(\tau)\left[\prod_{i\notin\{k,s\}}\sum_{t=1}^{\tau-1}F_i(t)\right], \tag{B1}$$

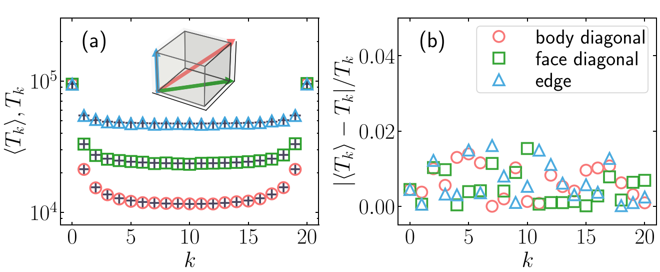

FIG. 7. (a) For standard random walk on a cube of 3D lattice with reflective boundary conditions, the MFPT $\langle T_k\rangle$ and the characteristic FPT T_k for sites along the body diagonal, face diagonal, and the edge of the cube. Each data point of $\langle T_k\rangle$ (empty triangles, squares, and circles) is the average over 20 000 simulations; T_k (the plus symbols) is calculated from $\mathbf{D}_k$ according to $T_k = -1/\ln(\lambda_k)$, where λ_k is the largest eigenvalue of $\mathbf{D}_k$. (b) The relative difference between $\langle T_k\rangle$ and T_k.

where $F_k(t)$ is the probability density of the FPT to site k. According to the analysis in Sec. II, $F_k(t)$ is an exponential function in the large FPT limit, replacing T_k by $\langle T_k\rangle$, and one has

$$F_k(t) \cong \frac{1}{\langle T_k\rangle}\exp\left(-\frac{t}{\langle T_k\rangle}\right).$$

Since $\tau \gg 1$, $\tau - 1 \cong \tau$, then the summation $\sum F_k(t)$ can be approximated as

$$\sum_{t=1}^{\tau} F_k(t) \cong 1 - \exp\left(-\frac{\tau}{\langle T_k\rangle}\right). \tag{B2}$$

Substituting the above equation into Eq. (B1), and considering $N \gg 1$ and that the condition $i \notin \{k, s\}$ can also be relaxed, the term in the square bracket can be approximated as

$$\begin{aligned}\prod_{i=1}^{N}\sum_{t}^{\tau}F_i(t) &\cong \prod_{i=1}^{N}\left[1-\exp\left(-\frac{\tau}{\langle T_i\rangle}\right)\right]\\ &\approx 1-\sum_i \exp\left(-\frac{\tau}{\langle T_i\rangle}\right)\\ &\quad+\frac{1}{2}\sum_{i\neq j}\exp\left(-\frac{\tau}{\langle T_i\rangle}-\frac{\tau}{\langle T_j\rangle}\right)-\cdots.\end{aligned} \tag{B3}$$

Note that the summation in the last term excludes the case $i = j$, as i appears only once in the product before the expansion. This also occurs in higher order terms, where the terms with identical indices are excluded. However, the number of those terms is about $1/N$ of all the terms, and since τ is typically much larger than $\langle T_i\rangle$ and that the most dominant term is the lowest order term, the above expression can be approximated by

$$\prod_{i=1}^{N}\sum_{t}^{\tau}F_i(t) \cong \exp\left[-\sum_{i=1}^{N}\exp\left(-\frac{\tau}{\langle T_i\rangle}\right)\right]. \tag{B4}$$

The above equation can be used to define a rescaling transformation to obtain the rescaled cover time χ from the original cover time τ:

$$\exp(-\chi) = \sum_{i=1}^{N}\exp\left(-\frac{\tau}{\langle T_i\rangle}\right) \tag{B5}$$

or

$$\chi = -\ln\sum_{i=1}^{N} e^{-\frac{\tau}{\langle T_i\rangle}}. \tag{B6}$$

Thus for a given set of $\{\langle T_i\rangle\}$, the rescaling relation between χ and τ is a monotonous deterministic function. Substituting Eqs. (B4) and (B5) back to Eq. (B1), and noting that from Eq. (B5)

$$d\chi/d\tau = \left[\sum_{k}^{N}\frac{1}{\langle T_k\rangle}\exp\left(-\frac{\tau}{\langle T_k\rangle}\right)\right]/\exp(-\chi),$$

one has

$$P(\tau) \cong \frac{1}{N} \sum_{k,s,\ k\neq s} F_k(\tau) \exp[-\exp(-\chi)]$$
$$= \exp[-\exp(-\chi)] \sum_{k=1}^{N} \frac{1}{\langle T_k \rangle} \exp\left(-\frac{\tau}{\langle T_k \rangle}\right) \tag{B7}$$
$$= \exp[-\exp(-\chi)] \exp(-\chi) d\chi/d\tau.$$

Since $P(\tau)d\tau = P(\chi)d\chi$, one has

$$P(\chi) \equiv \exp[-\chi - \exp(-\chi)], \tag{B8}$$

which is the rescaled distribution function.

APPENDIX C: DERIVATION OF THE RESCALED PARTIAL COVER-TIME DISTRIBUTION

In Sec. II, the partial cover-time distribution is given by

$$P_m(\tau) = \sum_{\{I_m\}} P(\tau | \notin \{I_m\}) Q(\tau, \{I_m\}), \tag{C1}$$

where $\{I_m\} = \{i_1, i_2, \cdots, i_m\}$ is a particular set of m sites, and $P(\tau | \notin \{I_m\})$ is the time distribution of covering all the other $N - m$ sites, regardless of whether it has been covered or not for the sites in $\{I_m\}$. The function $Q(\tau, \{I_m\})$ is the probability that the walker does not visit any of the sites in $\{I_m\}$ during time τ. After enumerating all possible configurations of $\{I_m\}$ by the summation $\sum_{\{I_m\}}$, the partial cover-time distribution $P_m(\tau)$ is then obtained.

$P(\tau | \notin \{I_m\})$ is the distribution for a random cover process. Using Eqs. (B5) and (B8), it can be written as

$$P(\tau | \notin \{I_m\}) = P(\chi | \notin \{I_m\}) \frac{d\chi}{d\tau}$$
$$= \exp[-\exp(-\chi)] \exp(-\chi) \frac{d\chi}{d\tau}\bigg|_{i\notin\{I_m\}}. \tag{C2}$$

Note that

$$\exp(-\chi)|_{i\notin\{I_m\}} = \sum_{i\notin\{I_m\}} \exp\left(-\frac{\tau}{\langle T_i \rangle}\right).$$

Since $m \ll N$, the summation of $N - m$ on the right hand side will be close to the summation over all the N terms, where the difference is on the order of m/N. Therefore, $\exp(-\chi)|_{i\notin\{I_m\}} \cong \exp(-\chi)$.

Thus

$$P(\tau | \notin \{I_m\}) = P(\tau) = P(\chi) \frac{d\chi}{d\tau}$$
$$= \exp(-\chi - e^{-\chi}) \frac{d\chi}{d\tau}, \tag{C3}$$

which is almost independent of $\{I_m\}$.

If the unvisited sites are uncorrelated, the probability Q can be explicitly obtained:

$$Q(\tau, \{I_m\}) = \prod_{i\in\{I_m\}} \left(1 - \sum_{t}^{\tau} F_i(t)\right), \tag{C4}$$

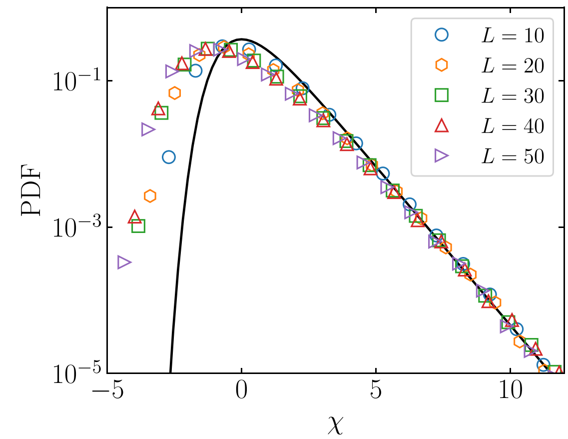

FIG. 8. Rescaled full cover-time distributions for 2D standard random walks with reflective boundaries. The cover-time distribution for each case is evaluated from sampling over 1×10^6 rounds. The symbols are the data rescaled with Eq. (7), and the thick black curve is the Gumbel distribution Eq. (9).

where $F_i(t)$ is the probability density of the FPT to site i. According to Eq. (B2), $Q(\tau, \{I_m\})$ can be expressed as

$$Q(\tau, \{I_m\}) = \prod_{i\in\{I_m\}} \exp\left(-\frac{\tau}{\langle T_i \rangle}\right). \tag{C5}$$

Equation (C1) for $P_m(\tau)$ can then be represented as

$$P_m(\tau) \sim \exp\left(-\chi - e^{-\chi}\right) \left[\sum_{\{I_m\}} \prod_{i\in\{I_m\}} \exp\left(-\frac{\tau}{\langle T_i \rangle}\right)\right] \frac{d\chi}{d\tau}.$$

The summation in the square brackets is over all possible combinations of m different sites out of the total N sites, for a total of

$$\binom{N}{m} = N \times \cdots \times (N - m + 1)/m!$$

terms. Note that the number of terms stated above excludes those with identical indices, which are in general only a small fraction, i.e., on the order of m/N. For $m \ll N$, their contributions can be neglected, and the summation in the square brackets can be approximated as

$$\frac{1}{m!} \left[\sum_i \exp\left(-\frac{\tau}{\langle T_i \rangle}\right)\right]^m = \frac{1}{m!} \exp(-m\chi). \tag{C6}$$

Then, the uncorrelated partial cover-time distribution is

$$P_m(\chi) = \frac{1}{m!} \exp\left[-(m+1)\chi - \exp(-\chi)\right], \tag{C7}$$

and the normalization condition is satisfied naturally.

When the unvisited sites have non-negligible but still small correlation, the approximation Eq. (C6) may be inaccurate. As a consequence, the value of m in Eq. (C7) has to be corrected to a smaller value m^*, while the same form Eq. (C7) of the partial cover time may still be valid.

APPENDIX D: THE NECESSITY OF NONCOMPACTNESS

In our derivation of the universal cover-time distributions and other theoretical treatments, noncompactness is an indispensable condition such that the correlation can be neglected. When there are non-negligible correlations, Fig. 4 shows slight deviation from the Gumbel distribution. It would be interesting to see more clearly the impact of broken noncompactness. Therefore, we calculate standard random walk on bounded 2D lattices with reflective boundary conditions, which is compact. The results are shown in Fig. 8. The deviation for small or negative χ is obvious. But for large positive χ, the agreement with the Gumbel distribution is still good. This is because for large positive χ, the cover time is long, where the effect of the correlation can be neglected, while for small or negative χ, the cover time is short, thus the correlation between subsequent visits is strong, and the approximation in the derivation of Eq. (4) becomes invalid, leading to the deviations.

---

[1] G. H. Weiss, *Aspects and Applications of the Random Walk* (North-Holland, Amsterdam, 1994).

[2] B. D. Hughes, *Random Walks and Random Environments* (Clarendon, Oxford, 1995).

[3] H. Qian and H. Wang, Continuous time random walks in closed and open single-molecule systems with microscopic reversibility, Europhys. Lett. **76**, 15 (2006).

[4] E. A. Codling, M. J. Plank, and S. Benhamou, Random walk models in biology, J. R. Soc. Interface **5**, 813 (2008).

[5] O. Bénichou and R. Voituriez, From first-passage times of random walks in confinement to geometry-controlled kinetics, Phys. Rep. **539**, 225 (2014).

[6] N. Masuda, M. A. Porter, and R. Lambiotte, Random walks and diffusion on networks, Phys. Rep. **716-717**, 1 (2017).

[7] I. Todhunter, *A History of the Mathematical Theory of Probability from the Time of Pascal to that of Laplace* (Cambridge University, Cambridge, England, 2006).

[8] A. Einstein, Über die von der molekularkinetischen theorie der wärme geforderte bewegung von in ruhenden flüssigkeiten suspendierten teilchen, Ann. Phys. (NY) **322**, 549 (1905).

[9] M. von Smoluchowski, Sur le Chemin Moyen Parcouru par les Molecules d'un Gaz et sur son Rapport avec la Théorie de la Diffusion, Bull. Int. Acad. Sci. Cracovie **7**, 202 (1906).

[10] M. C. Wang and G. E. Uhlenbeck, On the theory of the Brownian motion II, Rev. Mod. Phys. **17**, 323 (1945).

[11] R. Aleliunas, R. M. Karp, R. J. Lipton, L. Lovász, and C. Rackoff, Random walks, universal traversal sequences, and the complexity of maze problems, *20th Annual Symposium on Foundations of Computer Science (SFCS 1979)* (IEEE, New York, 1979), Vol. 1, pp. 218–223.

[12] J. D. Kahn, N. Linial, N. Nisan, and M. E. Saks, On the cover time of random walks on graphs, J. Theor. Probab. **2**, 121 (1989).

[13] A. M. Nemirovsky, H. O. Mártin, and M. D. Coutinho-Filho, Universality in the lattice-covering time problem, Phys. Rev. A **41**, 761 (1990).

[14] D. J. Aldous, On the time taken by random walks on finite groups to visit every state, Zeitschrift für Wahrscheinlichkeitstheorie und Verwandte Gebiete **62**, 361 (1983).

[15] H. S. Wilf, The editor's corner: The white screen problem, Am. Math. Mon. **96**, 704 (1989).

[16] G. M. Viswanathan, S. V. Buldyrev, S. Havlin, M. G. E. da Luz, E. P. Raposo, and H. E. Stanley, Optimizing the success of random searches, Nature (London) **401**, 911 (1999).

[17] O. Bénichou, C. Loverdo, M. Moreau, and R. Voituriez, Intermittent search strategies, Rev. Mod. Phys. **83**, 81 (2011).

[18] P. Grassberger, How fast does a random walk cover a torus? Phys. Rev. E **96**, 012115 (2017).

[19] M. L. Heuzé, P. Vargas, M. Chabaud, M. Le Berre, Y. J. Liu, O. Collin, P. Solanes, R. Voituriez, M. Piel, and A. M. Lennon-Duménil, Migration of dendritic cells: Physical principles, molecular mechanisms, and functional implications, Immunol. Rev. **256**, 240 (2013).

[20] V. Feller and W. Feller, *An Introduction to Probability Theory and its Applications* (Wiley, New York, 1968).

[21] A. Boneh and M. Hofri, The coupon-collector problem revisited, Purdue University Report No. 90-952, Computer Science Technical Reports, 1989 (unpublished).

[22] F. Wang and D. P. Landau, Determining the density of states for classical statistical models: A random walk algorithm to produce a flat histogram, Phys. Rev. E **64**, 056101 (2001).

[23] R. E. Belardinelli and V. D. Pereyra, Fast algorithm to calculate density of states, Phys. Rev. E **75**, 046701 (2007).

[24] M. Vergassola, E. Villermaux, and B. I. Shraiman, Infotaxis as a strategy for searching without gradients, Nature (London) **445**, 406 (2007).

[25] F. Wang and D. P. Landau, Efficient, Multiple-Range Random Walk Algorithm to Calculate the Density of States, Phys. Rev. Lett. **86**, 2050 (2001).

[26] C. Gkantsidis, M. Mihail, and A. Saberi, Random walks in peer-to-peer networks, *IEEE INFOCOM 2004* (IEEE, New York, 2004), Vol. 1, pp. 120–130.

[27] M. C. Santos, G. M. Viswanathan, E. P. Raposo, and M. G. E. da Luz, Optimization of random searches on regular lattices, Phys. Rev. E **72**, 046143 (2005).

[28] C. Avin and B. Krishnamachari, The power of choice in random walks: An empirical study, Computer Networks **52**, 44 (2008).

[29] A. N. Mian, R. Beraldi, and R. Baldoni, On the coverage process of random walk in wireless ad hoc and sensor networks, *The 7th IEEE International Conference on Mobile Ad-Hoc and Sensor Systems (IEEE MASS 2010)* (IEEE, New York, 2010), pp. 146–155.

[30] K. Li, Performance analysis and evaluation of random walk algorithms on wireless networks, Int. J. Found. Comput. Sci. **23**, 779 (2012).

[31] C. S. O. Yokoi, A. Hernández-Machado, and L. Ramírez-Piscina, Some exact results for the lattice covering time problem, Phys. Lett. A **145**, 82 (1990).
[32] D. J. Aldous, Threshold limits for cover times, J. Theor. Probab. **4**, 197 (1991).
[33] P. Erdős and A. Rényi, On a classical problem of probability theory, Magyar Tud Akad. Mat. Kutato Int. Közl **6**, 215 (1961).
[34] D. Aldous, *Probability Approximations via the Poisson Clumping Heuristic*, Applied Mathematical Sciences (Springer, New York, 1989).
[35] D. Belius, Gumbel fluctuations for cover times in the discrete torus, Probab. Theory Relat. Fields **157**, 635 (2013).
[36] M. Chupeau, O. Bénichou, and R. Voituriez, Cover times of random searches, Nat. Phys. **11**, 844 (2015).
[37] G. Maziya, L. Cocconi, G. Pruessner, and N. R. Moloney, Dynamically accelerated cover times, Phys. Rev. Res. **2**, 023421 (2020).
[38] B. F. Maier and D. Brockmann, Cover time for random walks on arbitrary complex networks, Phys. Rev. E **96**, 042307 (2017).
[39] E. Castillo, *Extreme Value Theory in Engineering*, Statistical Modeling and Decision Science (Elsevier, Amsterdam, 2012).
[40] C. Delattre and W. Dong, Fluid structure near heterogeneous surfaces, J. Chem. Phys. **110**, 570 (1999).
[41] S. Condamin, O. Bénichou, and M. Moreau, First-Passage Times for Random Walks in Bounded Domains, Phys. Rev. Lett. **95**, 260601 (2005).
[42] A. Zoia, M.-C. Néel, and A. Cortis, Continuous-time random-walk model of transport in variably saturated heterogeneous porous media, Phys. Rev. E **81**, 031104 (2010).
[43] S. Hwang, D.-S. Lee, and B. Kahng, Blind and myopic ants in heterogeneous networks, Phys. Rev. E **90**, 052814 (2014).
[44] C. Manzo, J. A. Torreno-Pina, P. Massignan, G. J. Lapeyre, M. Lewenstein, and M. F. Garcia Parajo, Weak Ergodicity Breaking of Receptor Motion in Living Cells Stemming from Random Diffusivity, Phys. Rev. X **5**, 011021 (2015).
[45] K. Cheng, J.-Q. Dong, L. Huang, and L. Yang, Cover-time distribution of random processes in granular gases, Phys. Rev. E **98**, 042109 (2018).
[46] L. Luo and M. Yi, Non-Gaussian diffusion in static disordered media, Phys. Rev. E **97**, 042122 (2018).
[47] L. Giuggioli, Exact Spatiotemporal Dynamics of Confined Lattice Random Walks in Arbitrary Dimensions: A Century after Smoluchowski and Pólya, Phys. Rev. X **10**, 021045 (2020).
[48] S. Hwang, D.-S. Lee, and B. Kahng, First Passage Time for Random Walks in Heterogeneous Networks, Phys. Rev. Lett. **109**, 088701 (2012).
[49] P. G. de Gennes, Kinetics of diffusion-controlled processes in dense polymer systems. I. Nonentangled regimes, J. Chem. Phys. **76**, 3316 (1982).
[50] J. Beirlant, Y. Goegebeur, J. Teugels, J. Segers, D. De Waal, and C. Ferro, *Statistics of Extremes: Theory and Applications*, Wiley Series in Probability and Statistics (Wiley, New York, 2006).
[51] K. R. Coutinho, M. D. Coutinho-Filho, M. A. F. Gomes, and A. M. Nemirovsky, Partial and Random Lattice Covering Times in Two Dimensions, Phys. Rev. Lett. **72**, 3745 (1994).
[52] B. Meyer, C. Chevalier, R. Voituriez, and O. Bénichou, Universality classes of first-passage-time distribution in confined media, Phys. Rev. E **83**, 051116 (2011).
[53] Starting from a given inner lattice site s, the walker moves to any of the six neighboring sites with identical probability $1/6$. If s is on the face and next step the walker moves out of the domain, it will then be reflected back by the face, say, to site i. Or equivalently, $\omega_{i\leftarrow s} = 1/3$, and the transfer probabilities to the other four neighbors on the face are all $1/6$. If s is on the edge, it has four neighbors, the two also on the edge each have a transfer probability $1/6$, while the other two neighbors each have a probability $1/3$. If s is at the corner, then it only has three neighbors; each has a transfer probability of $1/3$.
[54] P. Erdős and A. Rényi, On random graphs I, Publ. Math. Debrecen **6**, 290 (1959).
[55] A.-L. BarabÃ¡si and R. Albert, Emergence of scaling in random networks, Science **286**, 509 (1999).
[56] V. Tejedor, R. Voituriez, and O. Bénichou, Optimizing Persistent Random Searches, Phys. Rev. Lett. **108**, 088103 (2012).
[57] A. Izzet, P. G. Moerman, P. Gross, J. Groenewold, A. D. Hollingsworth, J. Bibette, and J. Brujic, Tunable Persistent Random Walk in Swimming Droplets, Phys. Rev. X **10**, 021035 (2020).
[58] M. F. Shlesinger and J. Klafter, Random walks in liquids, J. Phys. Chem. **93**, 7023 (1989).
[59] M. F. Shlesinger, Random searching, J. Phys. A: Math. Theor. **42**, 434001 (2009).
[60] V. Zaburdaev, S. Denisov, and J. Klafter, Lévy walks, Rev. Mod. Phys. **87**, 483 (2015).
[61] M. F. Shlesinger, *An Unbounded Experience in Random Walks with Applications* (World Scientific, Singapore, 2021).
[62] J. Pathak, B. Hunt, M. Girvan, Z. Lu, and E. Ott, Model-Free Prediction of Large Spatiotemporally Chaotic Systems from Data: A Reservoir Computing Approach, Phys. Rev. Lett. **120**, 024102 (2018).
[63] H. Fan, J. Jiang, C. Zhang, X. Wang, and Y.-C. Lai, Long-term prediction of chaotic systems with machine learning, Phys. Rev. Res. **2**, 012080(R) (2020).
[64] E. Ott, *Chaos in Dynamical Systems* (Cambridge University, New York, 2002).
[65] V. Latora, V. Nicosia, and G. Russo, *Complex Networks: Principles, Methods and Applications* (Cambridge University, New York, 2017).
[66] B. Rozemberczki, C. Allen, and R. Sarkar, Multi-Scale attributed node embedding, J. Complex Netw. **9**, cnab014 (2021).
[67] C. Klymko, D. F. Gleich, and T. G. Kolda, Using triangles to improve community detection in directed networks, *Proceedings of the the Second ASE International Conference on Big Data Science and Computing, BigDataScience*, 2014 (unpublished).
[68] H. Yin, A. R. Benson, J. Leskovec, and D. F. Gleich, Local higher-order graph clustering, *Proceedings of the 23rd ACM SIGKDD International Conference on Knowledge Discovery and Data Mining, KDD '17* (Association for Computing Machinery, New York, 2017), pp. 555–564.
[69] O. Bénichou, C. Chevalier, J. Klafter, B. Meyer, and R. Voituriez, Geometry-controlled kinetics, Nat. Chem. **2**, 472 (2010).
[70] A. Godec and R. Metzler, Optimization and universality of Brownian search in a basic model of quenched heterogeneous media, Phys. Rev. E **91**, 052134 (2015).
[71] K. Kim, J. Kyoung, and D.-S. Lee, Self-attracting walk on heterogeneous networks, Phys. Rev. E **93**, 052310 (2016).

[72] M. Dentz, D. R. Lester, T. Le Borgne, and F. P. J. de Barros, Coupled continuous-time random walks for fluid stretching in two-dimensional heterogeneous media, Phys. Rev. E **94**, 061102(R) (2016).

[73] J. Liu, J.-D. Bao, and X. Chen, Correlated continuous-time random walk in a velocity field: Anomalous bifractional crossover, Phys. Rev. E **102**, 062122 (2020).

[74] D. S. Grebenkov and L. Tupikina, Heterogeneous continuous-time random walks, Phys. Rev. E **97**, 012148 (2018).

[75] L. Cheng, A. AghaKouchak, E. Gilleland, and R. W. Katz, Non-stationary extreme value analysis in a changing climate, Clim. Change **127**, 353 (2014).

[76] I. Eliazar, R. Metzler, and S. Reuveni, Gumbel central limit theorem for max-min and min-max, Phys. Rev. E **100**, 020104(R) (2019).

[77] Z. Geng, Y. Zhang, B. Lu, J. Fan, Z. Zhao, and X. Chen, Network-synchronization analysis reveals the weakening tropical circulations, Geophys. Res. Lett. **48**, e2021GL093582 (2021).